

Orientational dynamics of the ionic organic liquid 1-ethyl-3-methylimidazolium nitrate

Hu Cang, Jie Li, and M. D. Fayer

Department of Chemistry, Stanford University, Stanford, California 94305

(Received 28 August 2003; accepted 30 September 2003)

Optical heterodyne-detected optical Kerr effect (OHD-OKE) experiments are used to study the orientational dynamics of the ionic organic liquid 1-ethyl-3-methylimidazolium nitrate ($\text{EMIM}^+\text{NO}_3^-$) over time scales from ~ 1 ps to ~ 2 ns, and the temperatures range from 410 to 295 K. The temperatures cover the normal liquid state and the weakly supercooled state. The orientational dynamics exhibit characteristics typical of normal organic glass-forming liquids. The longest time scale portion of the data decays as a single exponential and obeys the Debye–Stokes–Einstein relation. The decay of the OHD-OKE signal begins (~ 1 ps) with a temperature independent power law, t^{-z} , $z = 1.02 \pm 0.05$, the “intermediate power law.” The power law decay is followed by a crossover region, modeled as a second power law, the von Schweidler power law. The longest time scale decay is the exponential α relaxation. The intermediate power law decay has been observed in van der Waals supercooled liquids previously. These are the first such observations on an ionic organic liquid. The observation of the dynamical signatures observed in other liquids demonstrates that the orientational dynamics of ionic organic liquids are fundamentally the same as van der Waals liquids and supports the universality of the intermediate power law decay in the dynamics of complex liquids. Within the mode-coupling theory (MCT) framework, the MCT critical temperature T_C is estimated to be $T_C \cong 255$ K. © 2003 American Institute of Physics.
[DOI: 10.1063/1.1628668]

I. INTRODUCTION

Ionic organic liquids have attracted wide interest recently.^{1–8} They have potential important applications as environmentally friendly replacements for conventional organic solvents. Ionic organic liquids are also being used in the development of nanothrusters for space applications.⁹ As more ionic organic liquids become available, the range of potential applications will broaden. An understanding of both the dynamic and static properties of ionic organic liquids is needed. The study of the dynamical properties has just begun. Solvation dynamics in ionic liquids using steady state and time-resolved fluorescence experiments have been performed.^{1,7,8,10} Room temperature optical Kerr effect experiments on a number of ionic organic liquids have been conducted.^{11,12} Giraud *et al.* identified low-frequency modes associated with the imidazolium ring.¹¹ Hyun *et al.* studied a series samples of 1-alkyl-3-methylimidazolium bis[(trifluoromethyl)sulfonyl]imides with alkyl chain lengths of 2, 4, 5, 6, 8, and 10 carbons.¹² They found connections between high frequency librational motions and the local ordering of the liquids by comparing the spectral densities of various liquids. These two studies focus on the short time (less than a few ps) oscillatory dynamics (librations and internal low frequency modes) of the liquids. In addition, the nature of supercooled liquids and the glass transition of nonionic organic liquids and ionic inorganic molten salts have been studied intensively.^{13,14} Such studies generally involve longer time scales (> 1 ps). Studies have begun on ionic organic liquids as supercooled liquids, and a wide range of fragilities have

been observed.¹⁵ It is an interesting question as to how the dynamics of ionic organic liquids compare to those of van der Waals organic liquids.

In this paper, we report the dynamics of an ionic organic liquid over a wide temperature range in the normal liquid state and in the mildly supercooled state. The experiments are conducted using optical heterodyne-detected optical Kerr effect (OHD-OKE) experiments, which permit a broad range of time scales to be investigated. The OHD-OKE experiment measures the time derivative of the polarizability–polarizability correlation function, which is closely related to the orientational relaxation of a liquid.^{16,17}

Ionic organic liquids are very different from non-ionic organic liquids. The long-range Coulomb interactions in ionic organic liquids can lead to longer-range spatial correlations than those in comparable van der Waals organic liquids.¹⁸ Here we report OHD-OKE experimental results for the ionic organic liquid 1-ethyl-3-methylimidazolium nitrate ($\text{EMIM}^+\text{NO}_3^-$) over times from ~ 2 ps to ~ 2 ns, and temperatures ranging from 410 to 295 K. The melting point of $\text{EMIM}^+\text{NO}_3^-$ is ~ 313 K. Therefore, the study covers a temperature range from the normal liquid state to the weakly supercooled liquid state. It was found that $\text{EMIM}^+\text{NO}_3^-$ crystallizes at ~ 290 K, which prevents study further into the supercooled state.

Because the signal depends on the polarizability–polarizability correlation function, both the EMIM cation and the nitrate anion will contribute to the signal. Preliminary studies suggest that the EMIM⁺ produces the majority of the signal but that the contribution from the NO_3^- is non-

negligible. This is not surprising. The signal depends on polarizability anisotropy and the magnitude of the polarizability. EMIN^+ is an aromatic ring cation, and like other aromatics is both highly polarizable and highly anisotropic. However, NO_3^- also has significant π character and anisotropy.

Nonetheless, the results presented below demonstrate that the orientational dynamics of $\text{EMIM}^+\text{NO}_3^-$ on a long time scale behave in a very conventional manner, obeying the Debye–Stokes–Einstein equation as if EMIN^+ is undergoing orientational relaxation in a manner similar to a neutral aromatic ring compound. On all time scales the dynamics are very similar to five aromatic organic liquids that have been studied previously using the identical experimental methods and described in the context of mode-coupling theory (MCT).¹⁹

II. EXPERIMENTAL PROCEDURES

The ionic organic liquid 1-ethyl-3-methylimidazolium nitrate was purchased from Aldrich and used without further chemical purification. The samples were filtered through a 0.1 μm disk filter to remove dust and reduce scattered light. To make filtration possible, the filter syringe and the liquid were heated to reduce the viscosity. The samples were sealed under vacuum in 1 cm glass cuvettes. The cuvettes were held in a constant flow cryostat where the temperature was controlled to ± 0.1 K.

Optical heterodyne-detected optical Kerr effect spectroscopy^{20,21} used in the experiments^{17,19} is a type of pump–probe spectroscopy. The pump pulse creates a time-dependent optical anisotropy that is monitored via a heterodyne-detected probe pulse with a variable time delay. The OHD-OKE experiment measures the system's impulse response function, which is the time derivative of the polarizability–polarizability correlation function, which is closely related to the orientational relaxation of the molecules.^{16,17} In the experiments presented here, there are two species that give contributions to the signal, the EMIN^+ and the NO_3^- . Therefore, any collective motions of the species will influence the decay of the signal. Furthermore, in contrast to molecules studied previously, such as *o*-terphenyl, which is non-ionic and nonpolar, the strong Coulomb interactions in the sample could produce collective motions. The methods for the analysis of OHD-OKE data have been described in detail.^{20,21} The Fourier transform of the OHD-OKE signal is directly related to data obtained from depolarized light scattering,²² but the time domain OHD-OKE experiment can provide better signal-to-noise ratios over a broader range of times for experiments conducted on very fast to moderate time scales.

To observe the full range of liquid dynamics, at each temperature three sets of experiments were performed with different pulse lengths and delays. A mode-locked 5 kHz Ti:sapphire laser/regenerative amplifier system was used ($\lambda = 800$ nm) for both pump and probe. The pulse length was adjusted from < 100 fs to 100 ps to improve the signal-to-noise ratio. The shortest pulses were used for times 100 fs to ~ 12 ps. For longer times, a few ps to 600 ps, the pulses

were lengthened to 1 ps. For times from 100 ps to 5 ns, 100 ps pulses were used. The longer pulses produce an increase in signal amplitude for the longer time portions of the data. The scans taken over various time ranges always overlapped substantially, permitting the data sets to be merged by adjusting only their relative amplitudes.

To obtain the temperature scaling relations of the amplitudes of the two power laws, it is necessary to normalize the data to correct for the effects of laser intensity drift and sample density change when the temperature is changed. At $t = 0$, the OHD-OKE signal is overwhelmingly dominated by the instantaneous electronic response of sample. Because both the density changes caused by temperature variation and any laser intensity drift have essentially the same effect on the nuclear part and the electronic part of OHD-OKE signals, the OHD-OKE orientational relaxation data were normalized to the instantaneous electronic response at $t = 0$.

III. RESULTS AND DISCUSSION

The time dependence of the OHD-OKE signal was examined at 21 temperatures from 410 to 295 K. The melting point is ~ 313 K. The signal decays have a complex time dependence when examined from very short times to the long times. The functional form of the total decay will be discussed below. However, on the longest time scale, the decays at all temperatures studied are single exponentials. In the language of MCT, this is the final complete structural relaxation or α relaxation.^{23–25} The OHD-OKE experiment measures the time derivative of the polarizability–polarizability correlation function.¹⁶ To a first approximation the polarizability–polarizability correlation function may be considered to be the same as the orientational correlation function.¹⁷ Because the derivative of an exponential is the same exponential aside from a constant factor, the exponential decay gives the decay of the orientational correlation function directly.

A simple description of the orientational relaxation time in terms of the temperature and viscosity of a liquid is the Debye–Stokes–Einstein (DSE) equation,²⁶

$$\tau_\alpha = \frac{\eta f V_{\text{eff}}}{kT}, \quad (1)$$

where V_{eff} is the effective molecular volume, f is a factor that depends on the hydrodynamic boundary condition (stick or slip).^{27–30} Light scattering experiments,^{31–36} and transient grating optical Kerr effect experiments^{17,27} have shown that the single molecular orientation relaxation time τ_α can frequently be described very well by the DSE on the longest time scale of the relaxation.

Figure 1 displays a plot of the exponential decay time constants, τ_α versus η/kT . The temperature-dependent viscosity was obtained from the literature.³⁷ The inset shows one of the decays (410 K) on a semilogarithmic plot beginning at 30 ps, which is after the short-time-scale nonexponential dynamics have ended. The decay constant is 30 ps, and the decay is linear over more than four factors of e . According to Eq. (1), if the DSE equation is obeyed, the points in the main body of the figure should fall on a line.

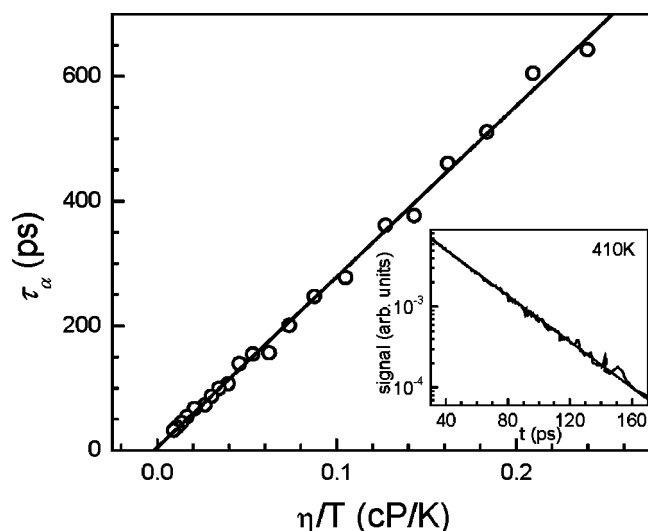


FIG. 1. The exponential decay constant for the slowest component of the decay plotted vs the viscosity (η) divided by the temperature (T). The fact that the points fall on a line shows that the data obey the Debye–Stokes–Einstein equation. The inset shows that the long-time portion of one of the decays is a single exponential.

The line through the data is a fit to the points. It is clear that the DSE equation is obeyed over the full range of temperatures studied.

Because the OHD-OKE experiment measures the collective orientational relaxation rather than the relaxation of a single solute molecule, the measured relaxation time may need to be corrected prior to comparison with the DSE equation. Keyes and Kivelson³⁸ have shown that the measured time τ_α is related to τ as

$$\tau_\alpha = (g_2/j_2)\tau, \quad (2)$$

where g_2 and j_2 are the static and dynamics orientation correlation parameters, and it is usually assumed that $j_2 \approx 1$. Transient grating OKE experiments¹⁷ found that $g_2 \approx 1$ for biphenyl.

For the qualitative comparison of interest here, we will assume that $g_2 \approx 1$ and $j_2 \approx 1$ for $\text{EMIN}^+\text{NO}_3^-$. Then the slope of the line in Fig. 1 yields fV_{eff} . It was determined that $fV_{\text{eff}} = 36 \text{ \AA}^3$. The effective volume of a solute molecule depends on the hydrodynamic boundary condition and the shape of the molecule. For symmetric ellipsoid molecules with stick boundary conditions, Perrin showed how³⁹ the effective volume is related to the molecular volume and the aspect ratio. Usually V_{eff} calculated by Perrin's formula is close to the molecular volume V_m , and for stick boundary conditions, $f=1$. It is found that when solute molecules have a size similar to the solvent molecules, slip boundary conditions are more appropriate than the stick boundary condition.³⁰ Youngren and Acrivos extended the DSE equation for ellipsoids with slip boundary conditions.⁴⁰

A simple model was used to calculate V_m , the molecular volume. The EMIM cation only was treated as an ellipsoid of revolution. Using CACHE software, the major and minor semi-axes were determined to be $a=3.7 \text{ \AA}$ and $b=2.2 \text{ \AA}$, respectively. The aspect ratio is $\rho \approx 0.6$. Using the Perrin formula for stick boundary conditions the effective volume is

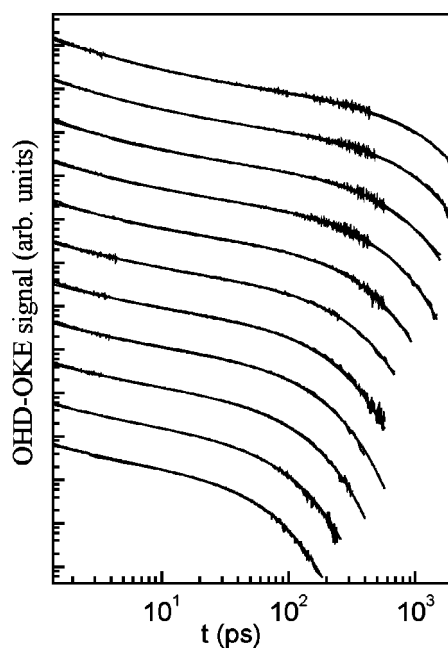


FIG. 2. Temperature dependent decays of the OHD-OKE data at 11 of the temperatures studied on a logarithmic plot. In addition, fits to the data using Eq. (3) are shown. The curves have been offset for clarity of presentation. The major temperature dependence is the slowing of the long-time-scale exponential relaxation as T is decreased. Starting with the topmost curve, the temperatures are: 295, 301, 307, 315, 325, 335, 345, 355, 370, 390, and 410 K.

$\sim 70 \text{ \AA}^3$. For slip boundary conditions, the correction coefficient λ is 0.54 for ellipsoids with $\rho \approx 0.6$.⁴⁰ Then, the effective volume under slip boundary conditions is 38 \AA^3 . Although the slip boundary condition results in better agreement, considering the simplicity of the model used here, both the stick and slip calculated V_{eff} 's are reasonably close to the experimentally measured $V_{\text{eff}} = 36 \text{ \AA}^3$.

The point of this exercise using the DSE equation is not that the proposed model of the rotating species is precisely correct. Detailed calculations on the structure of ionic organic liquids have begun to be performed.⁴¹ The model used here must be considered to be very approximate. The point is that $\text{EMIM}^+\text{NO}_3^-$ is behaving like a conventional van der Waals liquid. Many liquids composed of van der Waals molecules have been found to obey the DSE equation with measured effective volumes close to the calculated ones.^{17,27,31–33,35,36} The OHD-OKE decays will reflect collective orientational relaxation dynamics that might arise from strong interactions among the constituents of a liquid. For example, in the isotropic phase of liquid crystals, the long-time exponential decay of the OHD-OKE signal reflects the collective orientational relaxation of pseudonematic domains that exist in the liquid crystal.^{42–44} $\text{EMIM}^+\text{NO}_3^-$ appears to behave on the longest time scale as a conventional organic liquid.

Figure 2 displays data for 11 of the 21 temperatures studied from 295 K (top) to 410 K (bottom) on a log plot. The curves have been offset for clarity of presentation. The temperatures are given in the figure caption. The curves at all temperatures have the same general shape. The longest time portion of each curve is a single exponential decay. On a

logarithmic plot, an exponential decay appears as a knee and then a sharp drop. The decay constant, τ_α , for all 21 temperatures are given in Fig. 1. On shorter time scales, the curves are nonexponential and are apparently temperature independent. At times shorter than the exponential decays, the curves are parallel.

An important question is whether the strong Coulomb interactions in an ionic organic liquid fundamentally change the nature of the dynamics when compared to normal organic liquids. The EMIM cation is aromatic with side groups. In previous work using the same experimental technique, a universal functional form was found to describe the OHD-OKE data over a wide range of times and temperatures in five van der Waals supercooled liquids: orthoterphenyl, salol, dibutylphthalate, benzophenone, and 2-biphenylmethanol.^{19,45} These are also aromatic with various side groups. The following equation

$$F(t) = [pt^{-z} + dt^{b-1}] \exp(-t/\tau_\alpha) \quad (3)$$

fits the OHD-OKE signal decay of the five van der Waals liquids extremely well in both the normal and supercooled regimes. Equation (3) (Refs. 19 and 45) is related to dynamics predicted by mode coupling theory (MCT).^{46,47} t^{-z} is called the intermediate power law.^{19,45} z was found to be temperature independent and ranged from ~ 0.8 to ~ 1 for the five liquids.^{19,45} The intermediate power law spans a time range from ~ 1 ps to hundreds of ps or longer, depending on the temperature.^{19,45} The exponential decay $\exp(-t/\tau_\alpha)$ describes the long-time-scale α relaxation, with τ_α highly temperature dependent.^{19,45} The α relaxation is the final complete structural relaxation of the liquid.^{14,24,25,48-50} The second power law t^{b-1} is the crossover region between the intermediate power law and the α relaxation. It is called the von Schweidler power law in MCT and is the onset of the complete structural relaxation.^{46,47,51,52}

In addition to the data, Fig. 2 also shows fits to the data using Eq. (3). As is evident in Fig. 2, Eq. (3) fits the data extremely well. Fits to data taken at all 21 temperatures studied are equally good. In many of the curves at the very shortest times, 1-2 ps, there is some remnant of the oscillatory features that arise from excitation of low-frequency molecular modes by stimulated Raman scattering induced by the very short excitation pulses.^{11,49,53} In fitting the data, a global fitting procedure was used. In previous studies in which the liquids could be deeply supercooled, the α relaxation becomes so slow that von Schweidler power law becomes well separated from it.^{19,45} It is therefore straightforward to determine the exponent, b . This is also the case at the lowest temperatures studied here, but at higher temperatures, there is substantial error in determining b . Therefore, at each temperature, the full data set was fitted to Eq. (3). The values of b at the lower temperatures were independent of temperature with small random variation, which is consistent with previous measurements on van der Waals liquids.^{19,45} At the highest temperatures, the values of b varied randomly about the average value with variations of as much as a few tens of percent at the highest temperatures. From the individual fits, the average value of b was found, and this was fixed and the data were fit again. Because the intermediate power law at

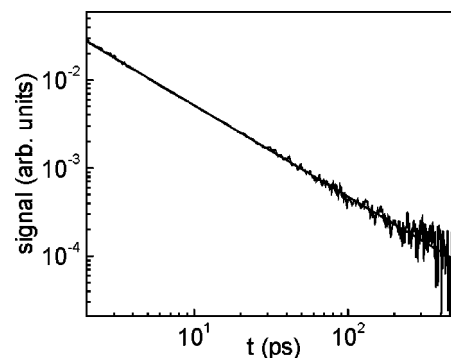


FIG. 3. Logarithmic plot of the power law portion of the data at the lowest temperature, 295 K, with the contributions from the long-time-scale exponential relaxation and the crossover region removed. The data are a power law over greater than two decades.

short time and the exponential decay at long time are well separated, this procedure did not significantly change the values associated with these components of the decay, but it did improve the consistency of the fits. The value of b is 0.87 ± 0.06 .

Figure 3 shows data on a logarithmic plot taken at one of the temperatures, 295 K, with the exponential component and the von Schweidler power law removed. The data show that the intermediate power law spans more than two decades in time. The line through the data is the power law $t^{-1.02}$. The data at all temperatures studied display the intermediate power law with temperature-independent exponent, $z = 1.02 \pm 0.05$ [see Eq. (3)].

It is clear from the data and fits presented in Figs. 2 and 3, that Eq. (3) fits the data extremely well over the full range of temperatures studied. As discussed above, Eq. (3) describes the functional form of the time dependence of five previously studied van der Waals liquids equally well.^{19,45} In all cases, the intermediate power law exponent, z , falls between ~ 0.8 and ~ 1 . Therefore, both the short- and long-time-scale dynamical behavior of the ionic organic liquid $\text{EMIN}^+\text{NO}_3^-$ is the same as nonionic aromatic liquids.

In addition to having the functional form of their decays described by Eq. (1), the five van der Waals liquids also obey three scaling relations predicted by MCT.^{24,45,47,54} These scaling relations are derived for supercooled liquids as they approach the MCT critical temperature, T_C . T_C is also called the ideal glass transition temperature because in standard MCT, the α relaxation is predicted to diverge at T_C .²⁴ However, experiments show that at T_C , the α relaxation is not infinitely slow.⁵⁵⁻⁵⁷ It is commonly accepted that T_C is the temperature at which the α relaxation changes from diffusive to activated.⁵⁶ Experiments show that T_C is typically 20% to 30% above the laboratory glass transition temperature, T_g .

Because $\text{EMIN}^+\text{NO}_3^-$ crystallizes somewhat below the melting point, the data are predominately taken above the melting point but do go somewhat into the supercooled region ($T < 313$ K). It is interesting to see if the data near and below the melting point obey the MCT scaling relations. The α -relaxation time, τ_α , scales with temperature as^{19,24}

$$\tau_\alpha \propto (T - T_C)^{-\gamma}, \quad (4)$$

with

$$\gamma = (a + b)/2ab, \quad (5)$$

and a and b are MCT parameters, which are related to each other via

$$\Gamma^2(1-a)/\Gamma(1-2a) = \Gamma^2(1+b)/\Gamma(1+2b), \quad (6)$$

where Γ is the gamma function. b is the von Schweidler power law exponent. The von Schweidler power law amplitude d scales with temperature as^{19,24}

$$d \propto (T - T_C)^\delta, \quad (7)$$

with

$$\delta = (a + b)/2a. \quad (8)$$

The two scaling relations given in Eqs. (2) and (5) come from the standard form of MCT. However, the standard form of MCT (lowest-order singularity solutions) does not predict the intermediate power law decay that has been observed in all five liquids that have been studied in detail previously or the intermediate power law observed in this study. There is a version of MCT, called the endpoint scenario (higher-order singularity solutions), that does predict the observed power law decay.^{47,54} However, the theory as it currently exists states that the end point scenario is a special case that would not be expected to apply to normal liquids.^{19,47,54} Nonetheless, the intermediate power law and the scaling relationship associated with it have been observed in the five supercooled van der Waals liquids.¹⁹ The intermediate power law amplitude p scales with temperature as,^{19,47,54}

$$p \propto (T - T_C)^{1/2}. \quad (9)$$

Each of the scaling relations contains the MCT critical temperature, T_C .²⁴

In this study data are available down to ~ 20 K below the melting point. In the previous liquids studied, data were used from $\sim T_C$ to the melting point or somewhat above it. Here we will use the data below the melting point and extend the range to 20 K above the melting point as a completely arbitrary cutoff. In Fig. 4(a) the τ_α data are plotted as $\tau_\alpha^{1/\gamma}$ versus T . γ is determined from Eq. (5); $\gamma = 1.94$. This is referred to as a rectification diagram.⁴⁹ If the scaling relation is obeyed, the points should fall on a line and extrapolate to T_C at $\tau_\alpha^{1/\gamma} = 0$. The data do fall on a line over the limited range of data used and yield a value of $T_C = 263$ K. In Fig. 4(b) the d data are plotted as $d^{1/\delta}$ versus T . δ is determined from Eq. (8); $\delta = 1.64$. Again the data fall on a line, showing that the scaling relation is obeyed and give a value of $T_C = 247$ K. From these results, $T_C \cong 255$ K. In the previous liquids studied, which had a much greater temperature range of data, the variations in the values of T_C given by the two scaling relations are less. Therefore, 255 K should be considered an estimate of T_C . Given this value of T_C , the glass transition temperature is very roughly estimated to be $T_g \cong 200$ K.

Figure 5 shows a rectification diagram for the third scaling relation, p^2 versus T . For the limited data employed, far from T_C , the scaling fails. The amplitude of the intermediate power law appears to show no temperature dependence. At

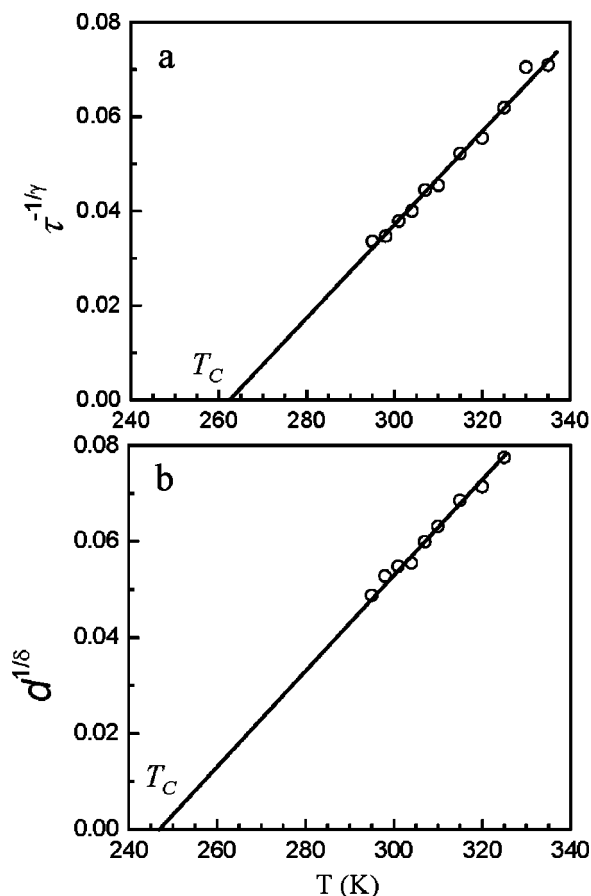


FIG. 4. Test of the first two MCT scaling relations. (a) The exponential decay time constant τ_α plotted as $\tau_\alpha^{-1/\gamma}$ vs T . The points fall on a line showing the scaling relation is obeyed and give $T_C = \sim 263$ K. (b) The amplitude of the von Schweidler power law d plotted as $d^{1/\delta}$ vs T . The points fall on a line showing the scaling relation is obeyed and give $T_C = \sim 247$ K.

this point it is unclear whether this is a real difference between ionic organic liquids and van der Waals fragile organic liquids or if it is a result of having too limited a range of data far from T_C . Other ionic organic liquids that are capable of being deeply supercooled are currently under study.

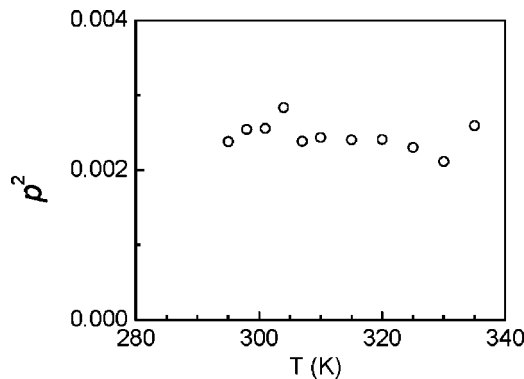


FIG. 5. Test of the third MCT scaling relation. The amplitude of the intermediate power law p is plotted as p^2 vs T . A line through the points should intersect the T axis to give T_C . The scaling relation is not obeyed.

IV. CONCLUDING REMARKS

Over a range of temperature from well above the melting point (~ 313 K) to somewhat into the supercooled region, the orientational dynamics of the ionic liquid 1-ethyl-3-methylimidazolium nitrate behaves in a manner that is essentially identical to organic aromatic van der Waals liquids. Optical heterodyne-detected optical Kerr effect experiments measured the dynamics from ~ 1 ps to ~ 2 ns. On the longest time scale, the data decay exponentially and the decay constants obey the Debye–Stokes–Einstein equation, which yields an effective volume that is similar to the molecular volume. The full time dependence of the data (derivative of the polarizability–polarizability correlation function) begins with a temperature-independent power law with exponent $z \sim 1$. This short-time power law is followed by a crossover region, another power law, that then becomes the long-time-scale exponential relaxation. The functional form of the decays is identical to the form previously found for five aromatic van der Waals liquids using identical experiments.^{19,45}

In the language of mode-coupling theory,^{23–25} the slowest decay is the α relaxation and the crossover region is the von Schweidler power law. The short-time power law, called the intermediate power law, has only recently been demonstrated to be an apparent universal feature of fragile glass-forming liquids^{19,45} and liquid crystals.^{58,59} In addition to having the same functional form as previously studied liquids and liquid crystals, the ionic organic liquid obeyed two of the three MCT scaling relations that the other liquids obeyed. It remains to be seen if the third relation will be obeyed in an ionic organic liquid that can be deeply supercooled.

The van der Waals organic liquids studied previously have weak intermolecular interactions. The nature of the intermolecular interactions in the ionic organic liquid is clearly very different. The ionic organic liquid is a two-component system composed of positive and negative charges. The liquid crystals may be considered to be intermediate in the strength and nature of the intermolecular interactions. The molecules are dipolar and rodlike. The intermolecular interactions are much stronger than those in the van der Waals liquids, but are in some sense weak compared to the Coulombic interactions of the ionic organic liquid. Nonetheless, the details of the temperature-dependent dynamics in all three types of liquids are virtually the same. Aspects of MCT seem to capture much of the nature of the dynamics, although the intermediate power law does not come from standard MCT results.^{19,47,54} While it may be too early to state definitively, the implication seems to be that liquids formed from molecules with a wide variety of properties display universal characteristics in their temperature-dependent dynamics.

ACKNOWLEDGMENTS

This work was supported by the National Science Foundation (Grant No. DMR-0088942) and the Air Force Office of Scientific Research (Grant No. F49620-01-1-0018). H.C.

was supported in part by a Franklin Veatch Memorial Fellowship, and J.L. was supported in part by a Stanford Graduate Fellowship.

- ¹J. A. Ingram, R. S. Moog, N. Ito, R. Biswas, and M. Maroncelli, *J. Phys. Chem. B* **107**, 5926 (2003).
- ²J. D. Holbrey and K. R. Seddon, *J. Chem. Soc. Dalton Trans.*, 2133 (1999).
- ³J. d. Andrade, E. S. Boees, and H. Stanssen, *J. Phys. Chem. B* **106**, 13344 (2002).
- ⁴P. A. Madden and M. Wilson, *J. Phys.: Condens. Matter* **12**, A95 (1999).
- ⁵M. C. C. Ribeiro, L. F. C. de Oliveira, and N. S. Goncalves, *Phys. Rev. B* **63**, 104303 (2001).
- ⁶T. Welton, *Chem. Rev.* **99**, 2071 (1999).
- ⁷R. Karmakar and A. Samanta, *J. Phys. Chem. A* **106**, 6670 (2002).
- ⁸R. Karmakar and A. Samanta, *J. Phys. Chem. A* **106**, 4447 (2002).
- ⁹J. Fernandez de la Mora, presented at the ACS National Meeting, New York, 2003 (unpublished).
- ¹⁰S. Arzhantsev, N. Ito, H. M., and M. Maroncelli, submitted to *Chem. Phys. Lett.*
- ¹¹G. Giraud, C. M. Gordon, I. R. Dunkin, and K. Wynne, *J. Chem. Phys.* **119**, 464 (2003).
- ¹²B.-R. Hyun, S. V. Dzuba, R. A. Bartsch, and E. L. Quitevis, *J. Phys. Chem. A* **106**, 7579 (2002).
- ¹³C. A. Angell, *Science* **267**, 1924 (1995).
- ¹⁴C. A. Angell, *J. Phys. Chem. Solids* **49**, 863 (1988).
- ¹⁵W. Xu, E. I. Cooper and C. A. Angell, *J. Phys. Chem. B* **107**, 6170 (2003).
- ¹⁶S. Ruhman, L. R. Williams, A. G. Joly, B. Kohler, and K. A. Nelson, *J. Phys. Chem.* **91**, 2237 (1987).
- ¹⁷F. W. Deeg, J. J. Stankus, S. R. Greenfield, V. J. Newell, and M. D. Fayer, *J. Chem. Phys.* **90**, 6893 (1989).
- ¹⁸G. Voth (private communication).
- ¹⁹H. Cang, V. N. Novikov, and M. D. Fayer, *J. Chem. Phys.* **118**, 2800 (2003).
- ²⁰D. McMorro and W. T. Lotshaw, *J. Phys. Chem.* **95**, 10395 (1991).
- ²¹D. McMorro, W. T. Lotshaw, and G. A. Kenney-Wallace, *IEEE J. Quantum Electron.* **24**, 443 (1988).
- ²²Y. Kai, S. Kinoshita, M. Yamaguchi, and T. Yagi, *J. Mol. Liq.* **65-6**, 413 (1995).
- ²³W. Götze, *Liquids, Freezing and Glass Transition* (Elsevier, Amsterdam, 1989).
- ²⁴W. Götze and L. Sjögren, *Rep. Prog. Phys.* **55**, 241 (1992).
- ²⁵G. Hinze and H. Sillescu, *J. Chem. Phys.* **104**, 314 (1996).
- ²⁶D. Kivelson, in *Rotational Dynamics of Small and Macromolecules*, edited by T. Dorfmueller and R. Pecora (Springer, Berlin, 1987).
- ²⁷R. S. Moog, M. D. Ediger, S. G. Boxer, and M. D. Fayer, *J. Phys. Chem.* **86**, 4694 (1982).
- ²⁸B. J. Berne and R. Pecora, *Dynamic Light Scattering* (Wiley, New York, 1976).
- ²⁹F. Perrin, *J. Phys. Radium* **5**, 497 (1934).
- ³⁰C. Hu and R. Zwanzig, *J. Chem. Phys.* **60**, 4354 (1974).
- ³¹G. R. Alms, D. R. Bauer, J. I. Brauman, and R. Pecora, *J. Chem. Phys.* **58**, 5570 (1973).
- ³²G. R. Alms, D. R. Bauer, J. I. Brauman, and R. Pecora, *J. Chem. Phys.* **59**, 5310 (1973).
- ³³G. R. Alms, D. R. Bauer, J. I. Brauman, and R. Pecora, *J. Chem. Phys.* **59**, 5321 (1973).
- ³⁴G. R. Alms, T. D. Gierke, and W. H. Flygare, *J. Chem. Phys.* **61**, 4083 (1974).
- ³⁵D. R. Bauer, G. R. Alms, J. I. Brauman, and R. Pecora, *J. Chem. Phys.* **61**, 2255 (1974).
- ³⁶D. R. Bauer, J. I. Brauman, and R. Pecora, *J. Am. Chem. Soc.* **96**, 6840 (1974).
- ³⁷K. R. Seddon, A. Stark, and M.-J. Torres, in *Clean Solvents*, ACS Symposium Series No. 819, edited by M. A. Abraham (American Chemical Society, Washington, D.C. 2002).
- ³⁸T. Keyes and D. Kivelson, *J. Chem. Phys.* **56**, 1057 (1972).
- ³⁹G. R. Fleming, J. M. Morris, and G. W. Robinson, *Chem. Phys.* **17**, 91 (1976).
- ⁴⁰G. K. Youngren and A. Acrivos, *J. Chem. Phys.* **63**, 3846 (1975).
- ⁴¹C. J. Margulis, H. A. Stern, and B. J. Berne, *J. Phys. Chem. B* **106**, (2002).
- ⁴²S. D. Gottke, D. D. Brace, H. Cang, B. Bagchi, and M. D. Fayer, *J. Chem. Phys.* **116**, 360 (2002).

- ⁴³S. D. Gottke, H. Cang, B. Bagchi, and M. D. Fayer, *J. Chem. Phys.* **116**, 6339 (2002).
- ⁴⁴H. Cang, J. Li, and M. D. Fayer, *Chem. Phys. Lett.* **366**, 82 (2002).
- ⁴⁵H. Cang, V. N. Novikov, and M. D. Fayer, *Phys. Rev. Lett.* **90**, 197401(4) (2003).
- ⁴⁶W. Götze, *J. Phys.: Condens. Matter* **2**, 8485 (1990).
- ⁴⁷W. Götze and M. Sperl, *Phys. Rev. E* **66**, 011405/1 (2002).
- ⁴⁸J. Chang and H. Sillescu, *J. Phys. Chem.* **101**, 8794 (1997).
- ⁴⁹G. Hinze, D. D. Brace, S. D. Gottke, and M. D. Fayer, *J. Chem. Phys.* **113**, 3723 (2000).
- ⁵⁰G. Hinze, D. Brace, S. D. Gottke, and M. D. Fayer, *Phys. Rev. Lett.* **84**, 2437 (2000).
- ⁵¹E. Bartsch, *Transp. Theory Stat. Phys.* **24**, 1125 (1995).
- ⁵²G. Li, G. M. Fuchs, W. M. Du, A. Latz, N. J. Tao, J. Hernandez, W. Götze, and H. Z. Cummins, *J. Non-Cryst. Solids* **172–174**, 43 (1994).
- ⁵³S. D. Gottke, D. D. Brace, G. Hinze, and M. D. Fayer, *J. Phys. Chem. B* **105**, 238 (2001).
- ⁵⁴W. Götze and R. Haussmann, *Z. Phys. B: Condens. Matter* **72**, 403 (1988).
- ⁵⁵W. Götze, *J. Phys.: Condens. Matter* **11**, A1 (1999).
- ⁵⁶P. G. Debenedetti and F. H. Stillinger, *Nature (London)* **410**, 259 (2001).
- ⁵⁷V. N. Novikov and A. P. Sokolov, *Phys. Rev. E* **67**, 031507 (2003).
- ⁵⁸H. Cang, J. Li, V. N. Novikov, and M. D. Fayer, *J. Chem. Phys.* (to be published).
- ⁵⁹H. Cang, J. Li, V. N. Novikov, and M. D. Fayer, *J. Chem. Phys.* **118**, 9303 (2003).